Chung Shan Medical Journal 2021; 32:21-30

Original Article

An analysis of the effects of breathing patterns on diaphragm motion

Cheng-Ming Tang[1, 5#], Cheng-Chang Lu[2, 3#], Chian-Yu Su[3], Yu-Chen Shen[4], Chun-Chao Chuang[2, 3*]

[1] *Institute of Oral Science, Chung Shan Medical University, Taichung, Taiwan*
[2] *Department of Medical Image, Chung Shan Medical University Hospital, Taichung, Taiwan*
[3] *Department of Medical Imaging and Radiological Sciences, Chung Shan Medical University, Taichung, Taiwan*
[4] *Department of Diagnostic Radiology, Linkou Chang Gung Memorial Hospital and Chang Gung University, Taoyuan, Taiwan*
[5] *Chung Shan Medical University Hospital, Taichung, Taiwan*

To investigate the correlation and feature changes of in vitro body contours and diaphragmatic displacement in different exhalation modes. We used the dynamic magnetic resonance imaging to sample the right thoracic sagittal image of 28 young volunteers in three modes of thoracic breathing, abdominal breathing, and free breathing. Measurements of the five external contours and diaphragmatic changes in the images were taken and their correlation and displacement characteristics were evaluated using their time-shift curves. We found that guided thoracic breathing has a more stable diaphragmatic shift. In the three breathing modes models, the height of the navel in the abdomen of the body contour displacement and the diaphragmatic shift has a high correlation. While the former three sections in the diaphragm section, the diaphragms near the posterior vertebrae had larger displacement amplitudes and the highest correlation with in vitro displacement. We recommend that the patient be able to have guided thoracic breathing to ensure stability of organ displacements. When the treatment or examination is performed, if the target area is located near the posterior abdominal wall of the thoracoabdominal junction, more displacement may need to be considered to ensure that the treatment target volume completely encompasses the tumor.

Keywords: diaphragm motion, IGRT, thoracic breathing, abdominal breathing

INTRODUCTION

In recent years, respiratory gating systems have found widespread application in the treatment of chest and abdominal tumors using radiotherapy, as these gating systems can track tumor movement, allowing radiation to be released only when the tumor enters the therapeutic target zone and thus significantly improving the accuracy of radiotherapy[1-3]. These gating systems are typically used under natural respiratory conditions, and they are suitable for patients with liver or lung tumors for which their positions are significantly affected by breathing motions[1-5]. For example, the CyberKnife systems have specialized calculation software for regulating and controlling the

* Correspondence: Chun-Chao Chuang
Address: No. 110, Sec. 1, Jianguo N. Rd., Taichung City 40201, Taiwan
Tel: +886-4-24730022 ext. 12365
E-mail: jimchao@csmu.edu.tw

correlation of internal and external signals[6-9]. When using systems, there are two available options when performing stereotactic body radiotherapy treatment on lung tumors:

1) The first option is inserting markers within or near the tumor, allowing positional changes of the tumor to be directly tracked using fluoroscopy. This method is highly accurate, but the invasive marker insertion procedure has a high risk of pneumothorax or other forms of harm.

2) The second method is using external respiratory surrogates to track external markers through photographic systems. This method is widely accepted in clinical practice, as it is simple, harmless, and effective in reducing organ movement tracking errors. However, methods based on internal and external displacement calculations are highly reliant on empirical data for converting external breathing waveforms into internal displacements[7&10].

For example, Ionascu et al. studied the correlation between abdominal movements and the motions of lung tumors[11]. Vedam et al. obtained similar results in their study on the correlation between displacements of the abdominal cavity wall and lung tumors[12]. A majority of studies uniformly found strong correlation between internal and external motions in the SI direction. The early works of Sharp[13], Ozhasoglu, and Murphy[14], as well as the later work of Mageras[15], uniformly concluded that the displacements of internal organs and the change in body contours are mismatched but that they display a correlation in displacement versus time plots. The correctional data obtained in these studies have been extremely useful in the application of clinical gating systems.

However, previous studies revealed that different breathing patterns can have significant effects on the motion of the diaphragm and the displacement characteristics of nearby organs. For example, Plathow et al. used dynamic magnetic resonance imaging (MRI) to study 20 patients with lung cancer to elucidate the correlation between the motion of tumors in different lung regions and that of the chest wall under various breathing patterns in an effort to evaluate lung tumor treatment plans[16]. They found that abdominal breathing (AB) causes relatively large tumor displacements in the SI direction, thoracic breathing (TB) has a larger effect on displacements in the AP direction, and non-specific breathing (NB) causes larger displacements in the RL direction. Nonetheless, most gating systems used in clinical applications are focused on collecting data from the abdominal region, with few of these systems tracking motions in the chest region. Studies that only focus on chest wall motions are thus unable to fulfill practical clinical requirements. Furthermore, the clinical application of radiotherapy gating systems is currently focused on regulation of the radiation initialization sequence. Investigations on displacement-induced changes in the segmentation of individual organs have received less attention by comparison. This information may be useful for reducing the margins of the therapeutic target volume.

The purpose of this study was to analyze the motion characteristics of the diaphragm and chest/abdomen contours when subjected to different breathing patterns. The results will provide a reference for clinical radiotherapy treatment planning and improve the tracking accuracy of respiratory gating systems.

Materials and Methods

Image processing

Twenty-eight healthy volunteers comprising 15 males and 13 females participated in this study. The entire experimental procedure was explained prior to the experiment, and each volunteer was personally instructed regarding how TB and AB should be performed. This study was granted clinical trial approval by the institutional review board.

This experiment used a 1.5 Tesla MRI outfitted with a two-channel body array coil for receiving chest and abdominal imaging signals. Test subjects were given breathing rhythm instructions through reflected projections. The MRI and respiratory parameters were as follows: 12 breathing cycles/min using the fast low angle shot scanning wave sequence, TR = 2.18 ms, TE = 0.74 ms, slice thickness = 10 mm, and field of view = 400 mm. In total, 511 mid-sagittal images of the right chest diaphragm were taken during each 2-min scan

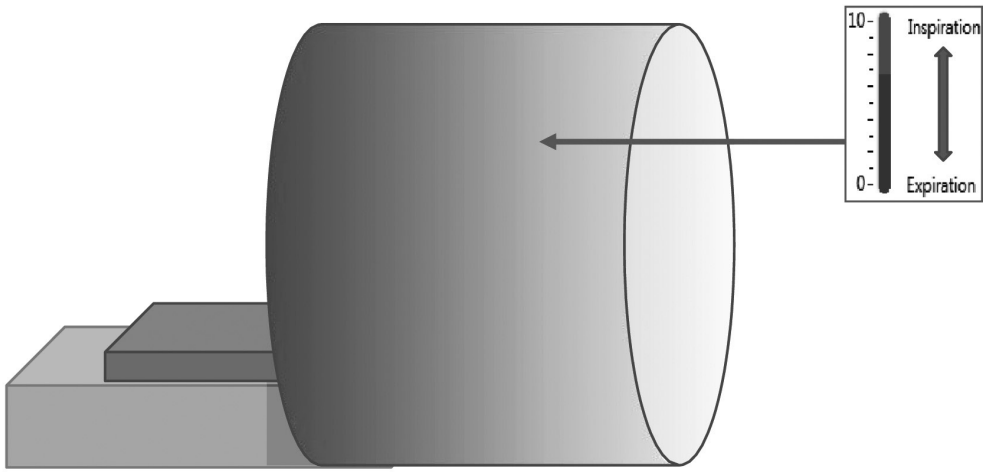

Figure 1. The figure showed experimental environment and right up picture showed the following instruction.

(Figure 1), which was the largest factory preset of the MRI machine. Three sets of MRI scans were performed for each test subject, and 24 breathing cycles were performed during each 2-min scan. These three scans were separately performed for TB, AB, and NB. In NB, no specific breathing pattern instructions were given to the test subjects, and no breathing rhythm guidance was provided through projections. Respiratory straps were attached at the xiphoid position during these scans to monitor whether the physiological breathing state of the test subject was stable and controlled. In the follow-up imaging analysis, the external respiratory strap was designated as the measurement point of the C segment.

Imaging analysis

The sagittal images of the chest were divided

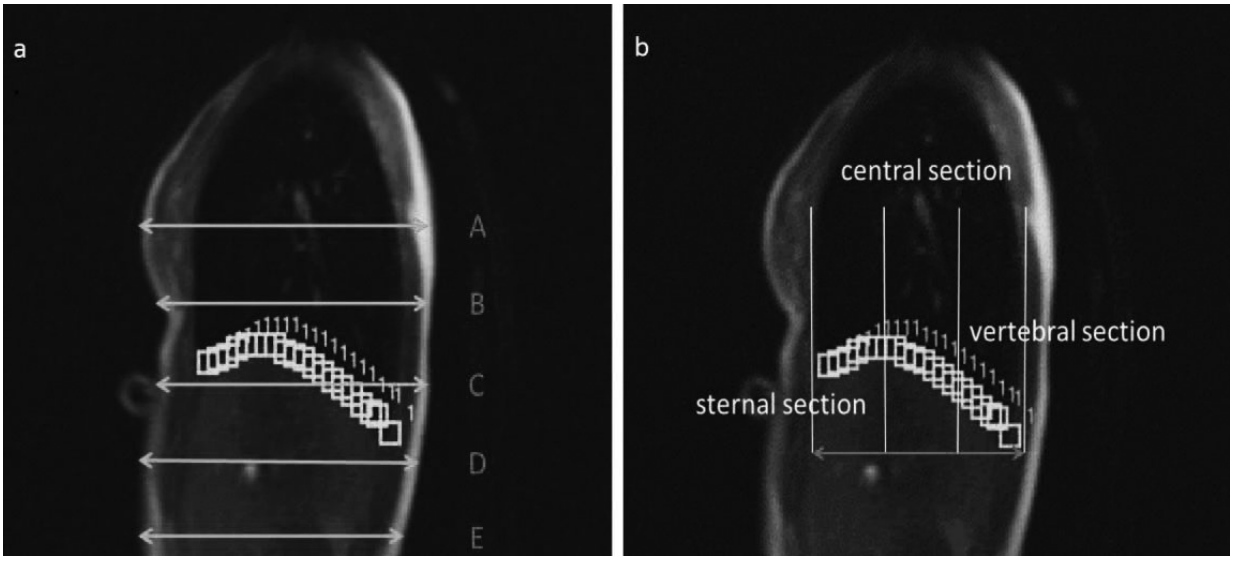

Figure 2. a. The sagittal images of the chest were divided into five segments as follows: A segment, position of the nipple; B segment, middle line between the A line at the nipple and the position at which the respiratory straps were placed during the MRI scan; C segment, position of the respiratory straps during the MRI scan (xiphoid); E segment, position at the height of the navel; and D segment, halfway between the C and E segments.

b. The diaphragm sampling marker points were then evenly divided into the sternal, central, and vertebral sections.

into five segments as Figure 2a. LabVIEW (Laboratory Virtual Instrumentation Engineering Workbench) was applied to analyze the time-dependent displacements of the five segments from the 511 images taken during each 2-min scan, with the values representing the external signals.

LabVIEW was also applied to sample the lung and liver boundaries, which were then taken as marker points of the diaphragm. Due to individual variations in body shape, 42–52 points were sampled along the diaphragm's delineation, and the average displacement versus plots of the diaphragm marker points were recorded using the 511 images taken over 24 breathing cycles. The diaphragm sampling marker points were then evenly divided into three groups (Figure 2b), i.e., the sternal, central, and vertebral sections. The average displacement versus time plots of the diaphragm markers of these three diaphragm sections were then recorded from the 511 images taken within 24 breathing cycles.

Statistical analysis

First, the average displacement versus time plots of the 28 test subjects' diaphragms were analyzed and compared. The distributions of amplitude maxima and minima were analyzed to obtain the turning points in diaphragm displacement that represent inhalation and exhalation, respectively; in this manner, the means and standard deviations of the three breathing patterns were compared. Then, the displacement versus time plots of the sternal, central, and vertebral sections of the diaphragm were analyzed and compared to obtain the average displacements and standard deviations of the individual diaphragm sections for each of the three breathing patterns.

Then, the displacement versus time plots of the five body contour segments were analyzed for each of the three breathing patterns, and the average displacements and standard deviations were compared. Finally, the displacements of the five body contour segments were compared with the average displacement of the diaphragm to study the relationship between these variables. The correlations between the displacements of the five external body contour segments and each of the three diaphragm sections were then investigated

Table 1. The relative position, amplitude of Diaphragm curve, amplitude of the diaphragm curve three segments and the displacement of the five body contour segments were measured in three breathing modes. (mm)

	AB	TB	NB
Diaphragm curve			
peak	23.99±2.60	17.34±1.72	11.44±1.38
valley	-28.96±6.74	-20.95±5.82	-15.49±4.25
amplitude	42.31±5.65	30.61±4.56	21.55±5.51
sternal section(D1)	29.40±6.36	24.33±5.55	16.91±5.99
central section(D2)	38.67±6.68	30.51±6.56	21.64±5.87
vertebral section(D3)	45.39±7.17	36.42±7.92	23.86±6.18
body contour segments			
A segment	4.52±0.81	9.37±2.15	3.46±1.38
B segment	3.83±1.04	9.04±1.69	2.77±1.17
C segment	3.30±0.75	7.29±1.34	2.25±0.77
D segment	4.10±0.92	7.75±1.42	2.41±0.78
E segment	9.52±1.25	9.06±1.50	3.66±1.23

individually for each of the three breathing patterns.

Results

In Table 1, the average value of the cyclical membrane displacement versus time plot of the 28 test subjects was set as the zero point for determining maximum and minimum amplitudes. The exhalation turning points (maximum amplitude) of the test subjects were 23.99 ± 2.60 mm for AB, 17.34 ± 1.72 mm for TB, and 11.44 ± 1.38 mm for NB, with significant differences observed among the three breathing patterns ($p < 0.001$). The minimum amplitude represents the inhalation turning point in the breathing cycle (corresponding to the diaphragm at its lowest position in the cycle and the lung at its maximum volume). These values were −28.96 ± 6.74, −20.95 ± 5.82, and −15.49 ± 4.25 mm for AB, TB, and NB, respectively, with the breathing patterns being significantly different from each other ($p< 0.001$). This study also calculated the average displacement of the diaphragm for each of the breathing patterns. The values were 42.31 ± 5.65 mm for AB, 30.61 ± 4.56 mm for TB, and 21.55 ± 5.51 mm for NB, with each of these average displacements being significantly different from the others.

This study further analyzed and compared the diaphragm displacement versus time plots of the D1 sternal section, D2 central section, and D3 vertebral section (Figure 3). The results shown in Table 1 indicate that the displacement was largest in the D3 vertebral section (AB: 45.39±7.17mm; TB: 36.42±7.92mm; NB: 23.86±6.18mm) and smallest in the D1 sternal section (AB: 29.40±6.36mm; TB: 24.33±5.55mm; NB: 16.91±5.99mm), with the differences among the three sections being significant.

We compared the correlation between respiratory breathing straps recorded information and c segment body contour. There is almost no difference between the two modes. So we can use the body contour of the image as in vitro respiratory information. Regarding the external signal, the displacement variability of the five body contour segments (A–E) was obtained using LabVIEW (show as Table 1). It was observed that the A segment has the largest average displacement (9.37±2.15mm) during TB, whereas the largest variability was observed in the E segment (9.52±1.25mm) (equivalent to the height of the navel) during AB. In NB, the variability of the five body contour segments was relatively small, but the A and E segments had the largest variabilities. It was also clear that the external body contour displacement was much smaller than the internal displacement of the diaphragm. Larger body contour displacement signals could only be observed at the E segment.

The displacement versus time plots of the

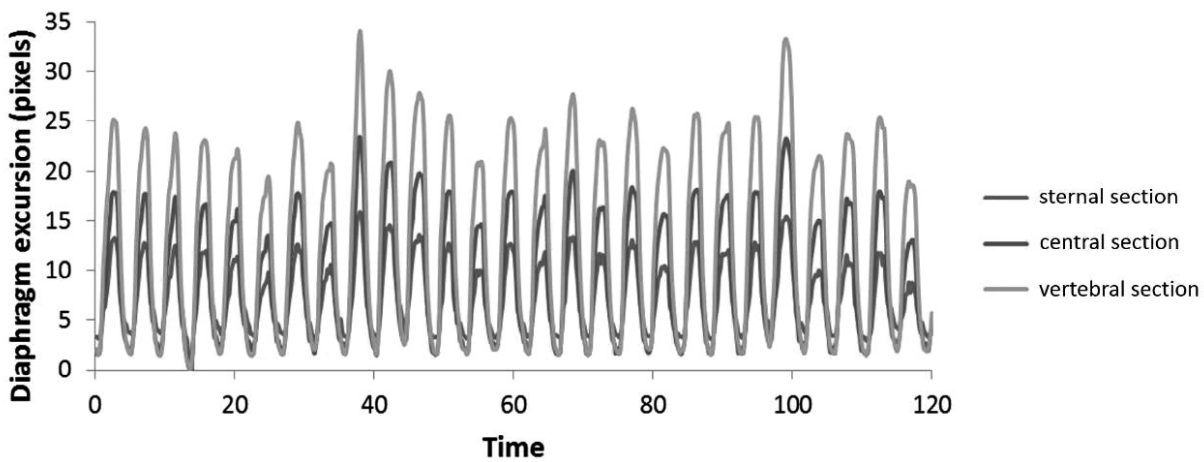

Figure 3. Three sections diaphragmatic displacement curve during abdominal breathing. The comparison of the displacement curves of three sections of diaphragms during the abdominal breathing in a subject, the displacement of the vertebral section> the central section> the sternal section.

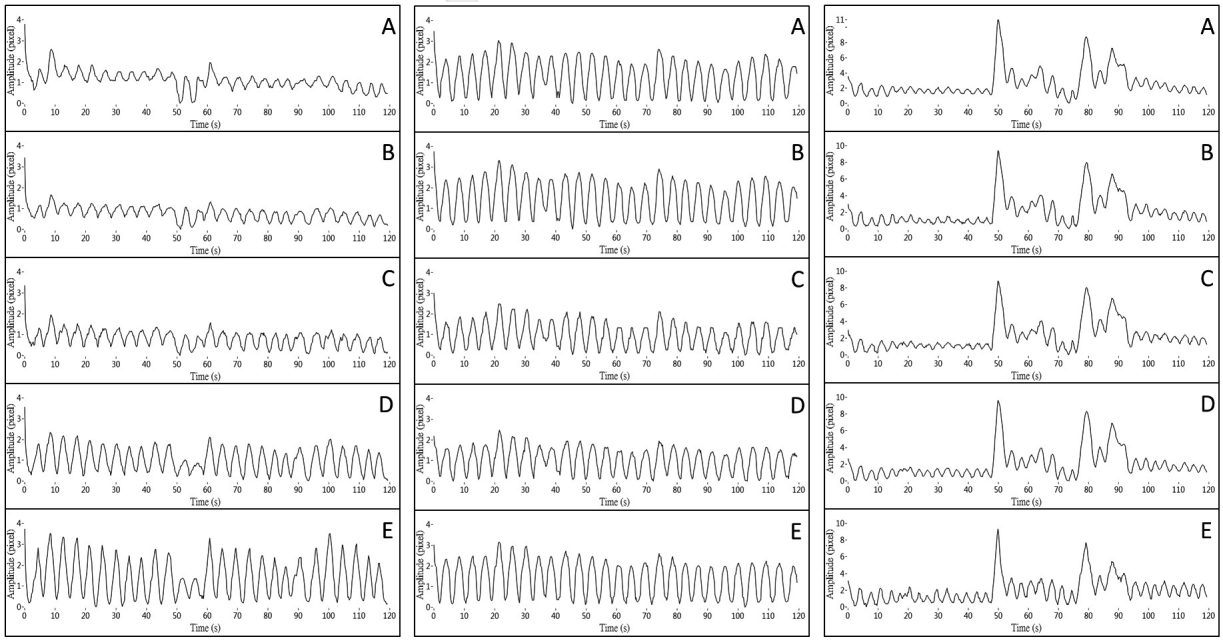

Figure 4. Five-segment displacement waveform of a subject in the abdominal breathing, thoracic breathing and non-specific breathing.

five external body contour segments recorded from a random test subject are shown in Figure 4. In abdominal breathing, it was found that the amplitudes of movement of the upper A, B, and C segments were relatively small, whereas the two segments closer to the abdomen had larger amplitudes. In thoracic breathing, the A and B segments on the thorax had larger amplitudes than the C and D segments, with an expansion in amplitude being noted in the E segment. The average of correlations between the various internal and external displacements are shown in Figure 5. During AB, these data illustrate that the E segment of the body contour had the highest correlation with the three diaphragm sections (E-D_1: 0.82±0.03; E-D_2: 0.83±0.05; E-D_3: 0.83±0.05), whereas lower correlations were observed for the three higher body contour segments. During TB, the correlation between the D1 sternal section and external body contours was low and highly variable, whereas the two other sections exhibited strong correlations with external body contour displacements, with the E

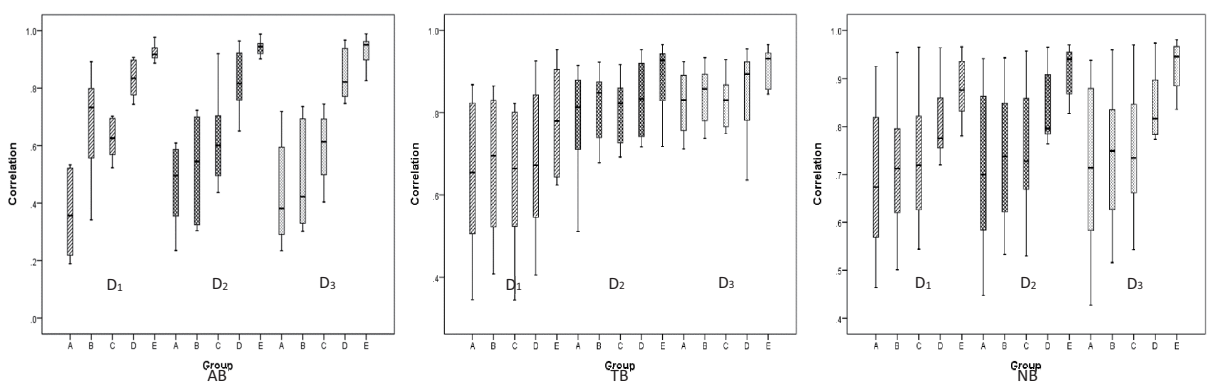

Figure 5. The box - shaped diagram of correlation between the 3 - sections diaphragm and the 5 - segments body contour.

segment displaying the highest correlation ($E\text{-}D_3$: 0.94±0.11). During NB, the five external segments had extremely small differences from one another (compared with Table 1, which shows that the A and E segments had larger variability amplitudes). A clear improvement in internal-external correlation was observed as the external markers approached the E segment near the navel. The waveform of the breathing cycle during NB, as compared with guided TB and AB, revealed larger variations in correlativity in the A–D segments, with the E segment being the only segment displaying stable correlativity.

Discussion

Kim et al. used projections to guide their test subjects' breathing rhythms and coordinated them with an RPM system to obtain external respiratory data, whereas diaphragm displacement was obtained using coronal MRI[17]. With these data, they compared the differences in breathing rhythm with and without the guidance system and found that the assistance of the gating system effectively increased respiratory stability, with the variability of diaphragm displacement being reduced by 67% using the guidance system. In this experiment, the diaphragm displacement versus time plots of the three breathing patterns of the 28 test subjects displayed the smallest deviations in peak values in TB, implying that TB has the highest uniformity at the exhalation turning point; with visual guidance, this deviation can be as small as 1.72 mm, which is 38% smaller than the 2.78-mm deviation observed with unguided NB. Although this improvement was somewhat smaller than that observed by Kim et al., it is speculated that this is because the 28 test subjects in this study were 20–30-year-olds with high levels of mental and physical fitness and consequently a higher level of baseline respiratory stability; thus, respiratory guidance only yields limited improvements in respiratory stability.

In a study by George et al., the respiratory variability of 24 patients with lung cancer was tracked using an RPM system, with these patients being given visual or auditory guidance or no guidance at all (NB)[18]. This study found that visual guidance reduced the standard deviation by 15% compared with NB, whereas auditory guidance led to a 20% decrease. Previous studies verified that 1) respiratory guidance can improve the accuracy of breath gating systems during radiotherapy and diagnostic examinations, 2) AV biofeedback respiratory guidance systems can effectively reduce irregularities in diaphragm movement and increase the regularity of breathing cycles, and 3) the use of respiratory gating is a highly effective method for reducing the positional offset of internal organs during CT and radiotherapy duty cycles[19-21]. However, studies examining differences linked with the use of respiratory guidance systems overlooked that every individual has a different method of breathing and that he or she may use different types of breathing, which may have different effects on the motion of internal organs. In this study, AB resulted in a higher level of variability in the respiration-induced displacements of internal organs than TB.

The diaphragm is the most important respiratory muscle. Stable breathing in a normal waking state proceeds through usage of the diaphragm; during stable NB, the diaphragm's contraction will decrease the height of the dome portion by 0.5–1.5 cm, but when breathing is conducted with effort, the dome may move by 6–10 cm in the inferior direction[22-23]. In this study, amongst the three breathing patterns studied, AB resulted in the largest average amplitude of movement in the diaphragm, reaching 42.31 ± 5.65 mm, whereas NB only resulted in an average amplitude of 21.55 ± 5.51 mm. This is mainly because the 12 cycles/min guided breathing rate is within the realm of deep breathing, whereas during unguided NB, some test subjects displayed clear signs of hurried breathing, with the breathing rate reaching 20 cycles/min for some individuals. In these cases, hurried breathing decreased the diaphragm's amplitude of movement while decreasing breathing stability. The ventilation efficiency of human bodies is at its highest when AB is utilized, but this also causes instability in the observed changes. Nevertheless, the stability of exhalation is relatively high, which explains why the observed standard deviation of peaks that represent exhalation was relatively small. TB was

found to be significantly more stable than NB or AB. TB has a higher level of stability with respect to internal displacements; therefore, the instability of internal changes may be reduced via guidance to regulate breathing rhythms and the appropriate selection of breathing patterns. If TB can be used during diagnostic or therapeutic procedures and the tracking of organs is specifically performed during exhalation, then the position of internal organs may be obtained with a higher level of stability and certainty.

By re-examining the diaphragm displacement versus time plots of the D1 sternal section, D2 central section, and D3 vertebral section, it is clear that the vertebral section had the highest displacement regardless of the breathing pattern utilized. This implies that the respiration-induced change in the diaphragm decreases as the diaphragm approaches the sternal end, whereas the respiration-induced change increases as the diaphragm approaches the vertebral end. This may be because the muscle groups that attach the diaphragm to the vertebra are longer and thus able to undergo larger displacements than the central and sternal sections. These results indicate that it is necessary in radiography to consider that if a coronal view scan takes a slice that is closer to the sternal end, the obtained diaphragmatic changes and organ displacements will be smaller, whereas a slice that is taken closer to the rear wall of the abdomen and back of the chest will reveal larger diaphragmatic displacements. The existence of this phenomenon has been verified by Plathow et al., who used dynamic MRI to study the coronal view images of 20 patients with lung cancer subjected to different breathing patterns[16]. Therefore, it is important to consider this point when planning radiotherapy treatments.

Based on our observations of the correlativity between the positional changes of the five external body contour segments and the three sections of the diaphragm (Figure 5), it was discovered that during AB, the motions of the three diaphragm sections displayed the highest correlation with the position of the navel (E segment), whereas the other segments have relatively low levels of correlation. Comparisons among the three sections of the diaphragm illustrated that they are equally correlated with each other, indicating that the time versus displacement waveforms of these diaphragm sections are essentially identical and only differ in amplitude. In AB, the abdominal muscles (rectus abdominis, abdominal oblique, and external oblique) are believed to consciously control the upward movement of the abdominal cavity and compression of the diaphragm. The thorax has a skeleton that restricts changes in its shape. During AB, the thorax is passive and restricted in motion, explaining why the displacement and correlativity of the navel height position are larger than those of the thorax. However, the box- plot demonstrated that the individual differences in thorax displacement were significant amongst the 28 test subjects. The differences in AB proficiency amongst the test subjects may have caused these large discrepancies. The trends observed in TB were clearly different from those in AB, as the positions of the five body contour segments and displacement of the diaphragm were more strongly correlated than observed in AB, albeit with a decreased level of correlation with the sternal section of the diaphragm, and large differences were noted between the sternal section and the two other diaphragm sections. This may be because the motive mechanism of TB begins with contraction of the intercostal muscles, which drives the sternum upward and forward to expand the thorax, thus increasing the volume of the thoracic cavity for inhalation, which in turn flattens the diaphragm. In this process, there will be a difference between the motion of the sternum and displacement of the diaphragm, thus decreasing the correlativity of the sternal end of the diaphragm.

In the work of Fernandes et al., who studied and analyzed cine-MRI data that were collected in 5-min intervals, it was found that 31% of patients had internal organ displacements that varied by at least 4 mm due to irregular breathing[24]. This type of change may be caused by the anxiety of the patients within the MRI apparatus; nevertheless, this is a naturally occurring change in breathing pattern. Regardless of whether an examination or treatment is being performed, a patient that is placed in unfamiliar environments, positioned

within confined spaces, or immobilized for a prolonged period may experience anxiety or restlessness. This study adopted a FLASH sequence, which has a shorter TE and TR than the cine-MRI technique adopted in the study by Fernandes et al. Thus, this study was able to collect data more rapidly and observe faster and more precise changes in respiration-related displacements.

Conclusions

During TB, the displacement changes of the body contour are correlated in a more stable manner with internal diaphragm displacements. During AB, a higher level of ventilation efficiency may be obtained (evidenced by larger diaphragm movement amplitudes and displacements), but this also leads to some respiratory instability. Only the navel position maintains a good level of correlativity, whereas the other segments are more strongly affected by the individual's proficiency in AB, thus resulting in large individual differences in correlativity. Therefore, when gated radiotherapy or examinations are being performed on a patient, the respiratory belt should be secured at the abdomen close to the navel height, at which strong correlation between internal and external motions can be obtained under most respiratory conditions. During respiration, organs are more strongly affected by movements of the diaphragm as their positions approach the vertebral end of the abdominal cavity. This in turn increases the correlation between external body contour changes and internal displacements. During examinations or treatments, if the target organ is positioned near the posterior abdominal wall of the chest-abdomen boundary, a larger level of displacement may need to be considered to ensure that the clinical target volume fully envelops the tumor.

References

1. Jiang S. Radiotherapy of Mobile Tumors. Seminars in Radiation Oncology. 2006;16(4):239- 248.
2. Shirato H, Shimizu S, Kitamura K, Nishioka T, Kagei K, Hashimoto S et al. Four- dimensional treatment planning and fluoroscopic real-time tumor tracking radiotherapy for moving tumor. International Journal of Radiation Oncology*Biology*Physics. 2000;48(2):435- 442.
3. Onimaru R, Shirato H, Fujino M, Suzuki K, Yamazaki K, Nishimura M et al. The effect of tumor location and respiratory function on tumor movement estimated by real-time tracking radiotherapy (RTRT) system. International Journal of Radiation Oncology*Biology*Physics. 2005;63(1):164-169.
4. Malinowski K, McAvoy T, George R, Dietrich S, D'Souza W. Incidence of Changes in Respiration-Induced Tumor Motion and Its Relationship With Respiratory Surrogates During Individual Treatment Fractions. International Journal of Radiation Oncology*Biology*Physics. 2012;82(5):1665-1673.
5. Malinowski K, McAvoy T, George R, Dieterich S, D'Souza W. Maintaining tumor targeting accuracy in real-time motion compensation systems for respiration-induced tumor motion. Medical Physics. 2013;40(7):071709.
6. Long S, Shang C, Evans G, Leventouri T. Variations of Cardiac Dose at Different Respiratory Status in CyberKnife Treatment Plans for Accelerated Partial Breast Irradiation (APBI). Medical Physics. 2015;42(6Part25):3521-3521.
7. Jung J, Song S, Yoon S, Kwak J, Yoon K, Choi W et al. Verification of Accuracy of CyberKnife Tumor-tracking Radiation Therapy Using Patient-specific Lung Phantoms. International Journal of Radiation Oncology*Biology*Physics. 2015;92(4):745-753.
8. Tu P, Nien H, Lee H, Wu C, Lin C, Lin C. The Dosimetric Impact of Moving Small Size Lung Tumor Using Helical Tomotherapy. Medical Physics. 2015;42(6Part24):3504-3504.
9. Kim Y, Jang S, Han J, Dong K, Chung W, Kim S. Motion and volume change of tumor tissue depending on patient position in liver cancer treatment with use of tomotherapy. Annals of Nuclear Energy. 2014;65:174-180.
10. Kim G, Hong J, Han S. Analysis of Correlation Coefficient Between Movements of Thoracoabdominal Tumors and External Respiration Using Image Guided Radiotherapy(IGRT). The Journal of the

Korea Contents Association. 2014;14(9):362-370.
11. Ionascu D, Jiang S, Nishioka S, Shirato H, Berbeco R. Internal-external correlation investigations of respiratory induced motion of lung tumors. Medical Physics. 2007;34(10):3893-3903.
12. Vedam S, Kini V, Keall P, Ramakrishnan V, Mostafavi H, Mohan R. Quantifying the predictability of diaphragm motion during respiration with a noninvasive external marker. Medical Physics. 2003;30(4):505-513.
13. Sharp G, Jiang S, Shimizu S, Shirato H. Prediction of respiratory tumour motion for real- time image-guided radiotherapy. Physics in Medicine and Biology. 2004;49(3):425-440.
14. Ozhasoglu C, Murphy M. Issues in respiratory motion compensation during external-beam radiotherapy. International Journal of Radiation Oncology*Biology*Physics. 2002;52(5):1389-1399.
15. MAGERAS G, YORKE E. Deep inspiration breath hold and respiratory gating strategies for reducing organ motion in radiation treatment. Seminars in Radiation Oncology. 2004;14(1):65-75.
16. Plathow C, Ley S, Fink C, Puderbach M, Hosch W, Schmähl A et al. Analysis of intrathoracic tumor mobility during whole breathing cycle by dynamic MRI. International Journal of Radiation Oncology*Biology*Physics. 2004;59(4):952-959.
17. Kim T, Pollock S, Lee D, O'Brien R, Keall P. Audiovisual biofeedback improves diaphragm motion reproducibility in MRI. Medical Physics. 2012;39(11):6921-6928.
18. George R, Chung T, Vedam S, Ramakrishnan V, Mohan R, Weiss E et al. Audio-visual biofeedback for respiratory-gated radiotherapy: Impact of audio instruction and audio-visual biofeedback on respiratory-gated radiotherapy. International Journal of Radiation Oncology*Biology*Physics. 2006;65(3):924-933.
19. Park Y, Kim S, Kim H, Kim I, Lee K, Ye S. Quasi-breath-hold technique using personalized audio-visual biofeedback for respiratory motion management in radiotherapy. Medical Physics. 2011;38(6Part1):3114-3124.
20. Gevaert T, Verellen D, Van de Vondel I, Engels B, Tournel K, Duchateau M et al. Treatment delivery time optimization of respiratory gated radiation therapy by application of audio-visual feedback. Physica Medica. 2011;27:S13.
21. Yamamoto T, Langner U, Loo B, Shen J, Keall P. Retrospective Analysis of Artifacts in Four-Dimensional CT Images of 50 Abdominal and Thoracic Radiotherapy Patients. International Journal of Radiation Oncology*Biology*Physics. 2008;72(4):1250-1258.
22. De Troyer A, Sampson M, Sigrist S, Macklem P. The diaphragm: two muscles. Science. 1981;213(4504):237-238.
23. Grimby G, Goldman M, Mead J. Respiratory muscle action inferred from rib cage and abdominal VP partitioning. Journal of Applied Physiology, 1976, 41(5): 739-751.
24. Fernandes A, Apisarnthanarax S, Yin L, Zou W, Rosen M, Plastaras J et al. Comparative Assessment of Liver Tumor Motion Using Cine–Magnetic Resonance Imaging Versus 4- Dimensional Computed Tomography. International Journal of Radiation Oncology*Biology*Physics. 2015;91(5):1034-1040.